A Role for Histone H4K16 Hypoacetylation in *Saccharomyces cerevisiae* Kinetochore Function

John S. Choy, Rachel Acuña, Wei-Chun Au, and Munira A. Basrai[1]
Genetics Branch Center for Cancer Research, National Cancer Institute, National Institutes of Health, Bethesda, Maryland 20892

ABSTRACT Hypoacetylated H4 is present at regional centromeres; however, its role in kinetochore function is poorly understood. We characterized H4 acetylation at point centromeres in *Saccharomyces cerevisiae* and determined the consequences of altered H4 acetylation on chromosome segregation. We observed low levels of tetra-acetylated and K16 acetylated histone H4 (H4K16Ac) at centromeres. Low levels of H4K16Ac were also observed at noncentromeric regions associated with Cse4p. Inhibition of histone deacetylases (HDAC) using nicotinamide (NAM) caused lethality in *cse4* and *hhf1-20* kinetochore mutants and increased centromeric H4K16Ac. Overexpression of Sas2-mediated H4K16 acetylation activity in wild-type cells led to increased rates of chromosome loss and synthetic dosage lethality in kinetochore mutants. Consistent with increased H4K16 acetylation as a cause of the phenotypes, deletion of the H4K16 deacetylase *SIR2* or a *sir2-H364Y* catalytic mutant resulted in higher rates of chromosome loss compared to wild-type cells. Moreover, H4K16Q acetylmimic mutants displayed increased rates of chromosome loss compared to H4K16R nonacetylatable mutants and wild-type cells. Our work shows that hypoacetylated centromeric H4 is conserved across eukaryotic centromeres and hypoacetylation of H4K16 at centromeres plays an important role in accurate chromosome segregation.

CENTROMERES serve as the chromosomal regions on which the kinetochores (*i.e.*, centromeric DNA and associated proteins) are assembled, multisubunit complexes essential for mediating **c**hromosome **t**ransmission **f**idelity (*ctf*) during cell division. Eukaryotes, such as budding yeast, have "point" centromeres, whereas fission yeast, fruit flies, and humans have "regional" centromeres. The point centromeres are small (~125 bp) and consist of CDE I–III, DNA elements that are highly conserved between each centromere. By contrast, regional centromeres are composed of repeated arrays of α-satellite DNA that range in size from ~0.1 to 5 Mb (Karpen and Allshire 1997). Despite the lack of sequence conservation, centromeres in all eukaryotes are assembled into a specialized chromatin that contains the centromere specific histone H3 variant (CenH3; Cse4p in budding yeast) (Ekwall 2007).

Several reports indicate that a unique chromatin structure is assembled at the centromere and pericentromeric regions in budding yeast. Work by Bloom and Carbon (1982) reported a specialized chromatin that extended several kilobases beyond the centromere sequence on both sides. Studies using fluorescence microscopy and chromosome conformation capture (3C) assays, revealed that the pericentromeric chromatin can form an intramolecular cruciform structure (pericentromeric loop) that has been proposed to be an important component of the mitotic spindle, balancing the forces between the kinetochore and spindle pole body (Bouck *et al.* 2008; Yeh *et al.* 2008; Anderson *et al.* 2009). In turn, disruption of nucleosomes by histone depletion (Saunders *et al.* 1990; Bouck and Bloom 2007), deletion of both *CAC1* and *HIR1* (Sharp *et al.* 2002), or deletion of *SPT4* (Crotti and Basrai 2004) result in declustering of kinetochores and compromised centromeric structure. Moreover, deletion of a single copy of histone H2A leads to polyploidy and mutants in the Hda1 deacetylase complex can suppress polyploidization (Kanta *et al.* 2006).

N-terminal covalent histone modifications modulate virtually all DNA-templated processes (Strahl and Allis 2000) and combinations of various histone modifications correlate with functional chromatin domains and activities (Millar and Grunstein 2006; Wang *et al.* 2009). Studies of regional centromeres showed that centromeric histones H3 and H4 are hypoacetylated, flanked by pericentromeric heterochromatin containing hypoacetylated H3 and H4 (Sullivan and Karpen

doi: 10.1534/genetics.111.130781
Manuscript received January 30, 2011; accepted for publication May 27, 2011
Supporting information is available online at http://www.genetics.org/content/suppl/2011/06/06/genetics.111.130781.DC1.
[1]Corresponding author: NIH/NCI Genetics, Bldg. 41, Room C629, 41 Center Drive, Bethesda, MD 20892. E-mail: basraim@nih.gov

2004). How histone H4 modifications affect kinetochore assembly and function is still not fully understood. Regional centromeres are composed of CenH3 nucleosomes interspersed with H3 nucleosomes that contain repetitive DNA, making it difficult to delineate the precise role of centromeric histone modifications. The point centromeres in *Saccharomyces cerevisiae* with a defined sequence and single centromeric nucleosome (Furuyama and Biggins 2007) provide a highly tractable system that bypasses these challenges.

Our work shows that there is a low level of acetylated histone H4 at the *S. cerevisiae* point centromere. Maintaining hypoacetylated H4 at the centromere is important for kinetochore function, as deregulated histone H4K16 acetylation causes growth defects in kinetochore mutants and chromosome missegregation. Taken together, we propose that hypoacetylated H4K16 is required for an optimal chromatin environment to ensure that the kinetochore mediates faithful chromosome segregation.

Materials and Methods

Strains and plasmids

Please refer to supporting information, Table S1 for a description of all yeast strains used. pRS316 (*CEN6 URA3*), pRS314 (*CEN6 TRP1*), pRS425 (*GAL1 2μ LEU2*), and pRS426 (*GAL1 2μ URA3*) were gifts from P. Hieter, University of British Columbia, British Columbia, Canada (Sikorski and Hieter 1989). pLG39 (*GAL1/10-HHF1 2μ URA3*) and pLG41 (*GAL1/10-HHT1 2μ URA3*) were provided by M. M. Smith, University of Virginia, Charlottesville, VA (Glowczewski *et al.* 2000). pSB816 (*GAL1/10-MYC-CSE4 2μ URA3*) was a gift from S. Biggins, Fred Hutchinson Cancer Center, Seattle, WA. pLP1197 (*GST-ESA1 in pRS425*) was a gift from L. Pillus, UC-San Diego, La Jolla, CA. pMB1193 (*GAL1 2μ SCM3 LEU2*) was generated by cloning *SCM3* in a pRS425 vector. pS116 (*pESC/URA/6XHIS-SAS2-FLAG*) and pS117 (*pESC/URA/6XHIS-sas2m1-FLAG*) were donated by J. L. Workman, Stowers Institute for Medical Research, Kansas City, MO (Osada *et al.* 2001). pDM607 (*sir2-H364Y*) and pDM608 (*SIR2*) were provided by D. Moazed, Harvard Medical School, Boston, MA (Tanny *et al.* 2004). pMB1434 and pMB1435 were generated by PCR-amplifying *SAS2* and *SAS2m1* using pS116 and pS117 as templates with primers including Hin*dIII*/Eco*RI* restriction sites and subcloning the respective fragments into pRS426 cut with the same enzymes. Cloning was verified by digestion and sequencing. For experiments, yeast strains were transformed with the aforementioned plasmids or the pBG1805 plasmid (*GAL1 URA3 His6X-3C-Protein A "zz" domain*) containing the desired mORF (*SAS2*, *SAS4*, and *SAS5*) obtained from Open Biosystems (Gelperin *et al.* 2005).

Growth assays

Strains grown on selective or rich media were used to prepare fivefold serial dilutions in water and 3.5 μl of each dilution was spotted on selective media with either 2% glucose or 2% raffinose and 2% galactose. Nicotinamide (NAM; Fluka Analytical, St. Louis, MO, CAS: 72340) was added at the indicated concentration where designated. Plates were incubated at the specified temperatures for 3–5 days and three independent transformants were tested for each strain.

Chromatin immunoprecipitation (ChIP) experiments

Cultures of each strain, starting OD ∼0.2, were grown until OD ∼0.8–1.0, typically at 30°, and cross-linked with formaldehyde for 30 min and processed essentially as described in Au *et al.* (2008). In experiments with *cse4-1*, cells were grown at 35° in 0 mM or 30 mM NAM from a starting OD ∼0.2 and cross-linked with formaldehyde for 30 min when cells reached OD ∼0.8. Glycine was added to a final concentration of 0.325 M, washed with 1× PBS, pelleted, frozen on dry ice, and stored. Pellets were resuspended in FA buffer (50 mM Hepes-NaOH pH 7.6, 150 mM NaCl, 1 mM EDTA, 1% Triton X-100, 0.1% Na-Deoxycholate) with Roche Protease inhibitor cocktail, 1 mM PMSF, 30 mM sodium butyrate. An equal volume of glass beads was added and samples were vortexed at 4° until >90% of cells were lysed as determined by microscopic inspection. Cells were separated from glass beads and sonicated to obtain sheared chromatin. Magnetic beads containing protein A or sheep antirabbit (Invitrogen) were preblocked with BSA, treated with antibodies to Myc (Santa Cruz), tAcH4 (Millipore), H4Pan (Millipore), H4K16 (ChIP grade from Active Motif), then added to chromatin samples for immunoprecipitation overnight at 4°. Beads were washed three times sequentially with FA buffer, HS-FA buffer (same as FA except with 500 ml NaCl), and two times with RIPA (10 mM Tris-Cl pH 8.0, 250 mM LiCl, 0.5% NP-40, 0.5% Na-Deoxycholate, 1 mM EDTA), and TE (Tris-Cl pH 8.0, 1 mM EDTA) before elution buffer (25 mM Tris-Cl pH 7.6, 10 mM EDTA, 0.5% SDS) was added to resuspend the beads and incubated overnight at 65° to reverse cross-links. Beads were removed and the samples treated with proteinase K at 55° for ∼4 hr, phenol chloroform extracted or a Qiagen PCR clean up kit used to isolate DNA. We used the relative quantification method of qPCR with Sybr Green (ABI) and calculated enrichment from $2^{-(CT(IP)-CT(mock))}$ (Figures 1, 3, S1, S3). Alternatively, we analyzed ChIP DNA samples with standard PCR and 1.5% agarose gel electrophoresis containing EtBr. Gels were imaged and DNA products were quantified using GeneSnap and GeneTools from SynGene, respectively. The ratio of H4K16Ac and/or tAcH4 products to pan H4 products were plotted (Figures 3C, 4B, S2, S3, S4, S5). Primer pairs to each region assayed were designed to amplify DNA fragments ∼200–300 bp in length. Primer sequences are available upon request.

Chromosome loss assays

Assays were performed essentially as previously described in Hieter *et al.* (1985). Strains containing the nonessential chromosome fragment (CF) were grown on medium selective

for the CF and the selectable marker on the plasmid that was being assayed. Cells were plated on SC media with limiting adenine and incubated at 30° for 5–7 days. Chromosome loss was determined by counting colonies that were at least half-sectored, indicating loss of the CF during the first cell division. Three transformants for each strain were assayed; ~1–2000 colonies were counted.

Results

Low levels of acetylated histone H4 are present at centromeric chromatin

A distinct pattern of histone H3 and H4 modifications has been reported for regional centromeres (Hayashi *et al.* 2004; Sullivan and Karpen 2004). Considering the role of H4 acetylation in chromatin structure, we explored the possibility that there were acetylated H4 isoforms at centromeric (~200 bp centered on the CDE I–III sequences) chromatin in *S. cerevisiae*. Using chromatin immunoprecipitation (ChIP) with an antibody that recognizes all forms of N-terminal acetylated histone H4 (tAcH4), we observed that the centromere region of chromosome III (CEN III) contains lower levels of tAcH4 (~3-fold less) compared to *SNR189* (+CTL), a region with hyperacetylated histone H4 (Liu *et al.* 2005) (Figure 1). Our results for tAcH4 are derived from four different primer pairs that amplify the core centromere sequence (C1 and C2) and the 200-bp regions immediately upstream and downstream of the centromere (C3 and C4). As a negative control, we analyzed the HML locus (−CTL), which is known to contain hypoacetylated H4 (Rusche *et al.* 2003). As expected, we found virtually no tAcH4 at HML, indicated by <1-fold enrichment (Figure 1B). Low levels of tAcH4 were also present in the pericentromeric region ~300 bp downstream of the centromere (R1) compared to the region ~300 bp upstream of the centromere (L1). The latter region overlaps with an uncharacterized open reading frame (YCL001W-B) and this may contribute to the higher level of tAcH4. We also observed a low level of tAcH4 (~3-fold less than *SNR189*) at the core centromere of chromosome VI (Figure S1). All regions analyzed were normalized to total histone H4 (modified and unmodified) using an antipan H4 antibody to account for any differences in nucleosome positioning or potential differences in ChIP efficiencies at the centromere compared to noncentromeric regions as previously described (Camahort *et al.* 2009). We have provided examples of the differences in the percentage of input for pan-H4 at CEN III and VI compared to noncentromeric regions (Figure S2). We refer to the lower levels of tAcH4 at the centromere region as hypoacetylated. To confirm that the domain of hypoacetylated H4 overlapped with the centromere region, we performed ChIP assays for Cse4p (Furuyama and Biggins 2007). Our results showed that Myc-Cse4p was highly enriched (on average ~20-fold enrichment) in the same C2 region of CEN III containing hypoacetylated H4 but not in the flanking regions L1 and R1 or at HML (−CTL) (Figure 1C).

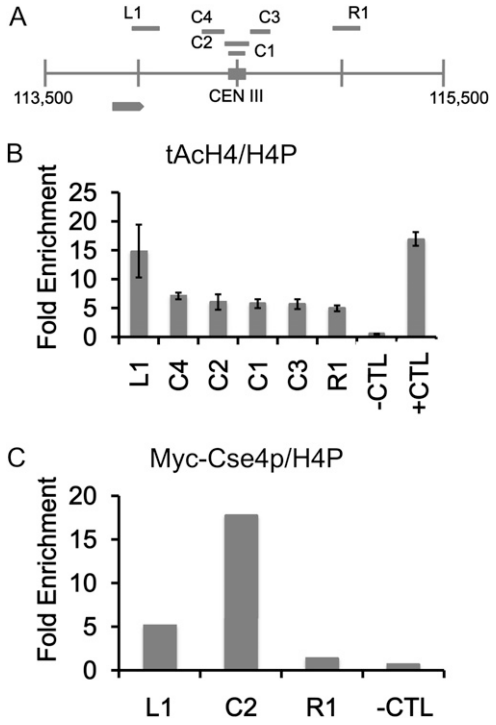

Figure 1 Low levels of acetylated H4 are observed at the centromere. Chromatin immunoprecipitation (ChIP) experiments were performed with asynchronously grown wild-type strains expressing Myc-Cse4p (YMB6955). (A) Diagram of centromere (CEN) (C1–4) and pericentromeric regions (L1 and R1) on chromosome III analyzed by ChIP. Solid square represents the CEN III sequence and each vertical line from chromosomal coordinate 113,500 to 115,500 denotes 500-bp increments. Gray arrow represents an uncharacterized open reading frame (YCL001W-B). (B and C) ChIP with antibodies that recognize acetylated isoforms of acetylated histone H4 (tAcH4) to measure the levels of H4 acetylation at centromeric (C1–4) regions or to Myc to measure levels of Myc-Cse4p at centromeric C2 region and pericentromeric (L1 and R1) regions by quantitative PCR. HML serves as a hypoacetylated H4 control (−CTL) region and *SNR189* (SNR) (Chr III: 178729–178589) is a hyperacetylated H4 control (+CTL) region. ChIP for total H4 was performed with antibodies to pan H4 (H4P) that recognize modified and unmodified forms. Bar graphs in B show mean fold enrichment for tAcH4 normalized to total H4 from three biological replicates with error bars showing standard error of the mean. Bar graphs in C show mean fold enrichment for Myc-Cse4p normalized to total H4 from two biological replicates.

We wanted to determine whether chromosomal sequences were important for the observed hypoacetylated histone H4 at the centromere or whether the centromere sequence alone was sufficient. Thus, we examined tAcH4 at a minimal centromere on a pBluescript-based plasmid (pRS316) with heterologous sequences on both sides. An ARS element and the *URA3* marker are downstream, and bacterial sequences are upstream of the centromeric sequence (CEN VI) (Figure S3). We introduced pRS316 into a *S. cerevisiae* strain in which the endogenous CEN VI is replaced with CEN XI and performed ChIP experiments to determine the level of tAcH4 at the plasmid-based CEN VI. As in Figure 1 we used two different primer pairs that amplify the core centromere sequence (pC1 and pC2) and two different primer pairs that amplify the 200-bp regions immediately upstream and

downstream of the centromere (pL and pR). Consistent with a centromere-dependent pattern, we observed that there were ~2-fold lower levels of tAcH4 at CEN VI than at *SNR189* (+CTL) (Figure S3), similar to that observed for endogenous CEN III (Figure 1B).

Mutants in CSE4 and HHF1 are sensitized to nicotinamide (NAM)

The results of our ChIP experiments for tAcH4 suggested that similar to regional centromeres, histone H4 at the centromere in *S. cerevisiae* is hypoacetylated. Acetylation of specific lysine residues on H3 and H4 can lead to different functional outcomes (Millar and Grunstein 2006; Wang *et al.* 2009). Levels of K16 acetylation on H4 is a major determinant in regulating chromatin structure in yeast and metazoans (Shogren-Knaak and Peterson 2006). Therefore, we investigated whether altering H4K16 acetylation might exhibit synthetic interactions with kinetochore mutants. Several studies have shown that NAM inhibits NAD-dependent HDACs, including Sir2p (Sanders *et al.* 2007), and leads to higher levels of acetylated H4K16 (H4K16Ac) (Dang *et al.* 2009). The centromeric nucleosome contains Cse4p and H4, and the C-terminal histone fold domain of Cse4p has been shown to be important for interaction with H4 (Smith *et al.* 1996; Glowczewski *et al.* 2000). Temperature-sensitive (ts) alleles of *cse4-1*, *cse4-111*, and *hhf1-20* have chromosome segregation defects. The *cse4-1* and *cse4-111* strains have mutations in the histone fold domain and the *hhf1-20* strain contains mutations near the DNA binding region and helix 3 of the histone fold domain that are thought to weaken interactions with Cse4p (Stoler *et al.* 1995; Smith *et al.* 1996; Glowczewski *et al.* 2000). If low levels of H4K16Ac are important for kinetochore function, we predict that *cse4* and *hhf1-20* mutants treated with NAM would result in enhanced growth defects. We found that *cse4-1* and *cse4-111* displayed an increase in temperature sensitivity to NAM at 33° and 30°, respectively, but wild-type cells remained unaffected at both temperatures (Figure 2A). Similar to *cse4* mutants, the histone H4 mutant *hhf1-20* was also sensitive to NAM at 30° (Figure 2B). If the growth defects observed in *cse4* and *hhf1-20* mutants were mediated through modulating H4K16 acetylation, then we would predict that mutants in which lysine 16 is changed to glutamine (H4K16Q), an acetylmimic or an arginine (H4K16R) that is nonacetylatable, should not result in decreased fitness. On the other hand, if the NAM effects were a result of H4 independent pathway(s) then H4K16Q and H4K16R mutants might both show enhanced growth defects in the presence of NAM. Consistent with NAM inihibition acting on H4K16 acetylation, we observed no growth defects for these mutants when grown on NAM at 30° or 35° (Figure 2B). To determine whether the growth defects in *cse4-1*, *cse4-111*, and *hhf1-20* strains were a general toxicity of kinetochore mutants to NAM, we tested the kinetochore mutants, *ndc10-1*, *mif2-3*, *mcm21Δ*, and *ctf19Δ*. A mild growth defect was observed in *ndc10-1* strain at 30° (note that the *ndc10-1* strain is inviable above 30°) but no growth defects were observed for *mif2*-3, *ctf19*Δ, or *mcm21*Δ to NAM at 30°, 33° and 35° (Figure 2C).

Low levels of H4K16Ac are present at the centromere and noncentromeric regions enriched for Cse4p

The low level of tAcH4 at the centromere together with the sensitivity of *cse4* and *hhf1-20* mutants to NAM prompted us to measure the levels of H4K16Ac at the centromere (Shahbazian and Grunstein 2007). We performed ChIP assays with an antibody that recognizes acetylated histone H4K16 and four different primer pairs for CEN III (C1–C4) as described in Figure 1. We determined that all four regions corresponding to the centromere region of chromosome III and the upstream (L1) and downstream regions (R1)

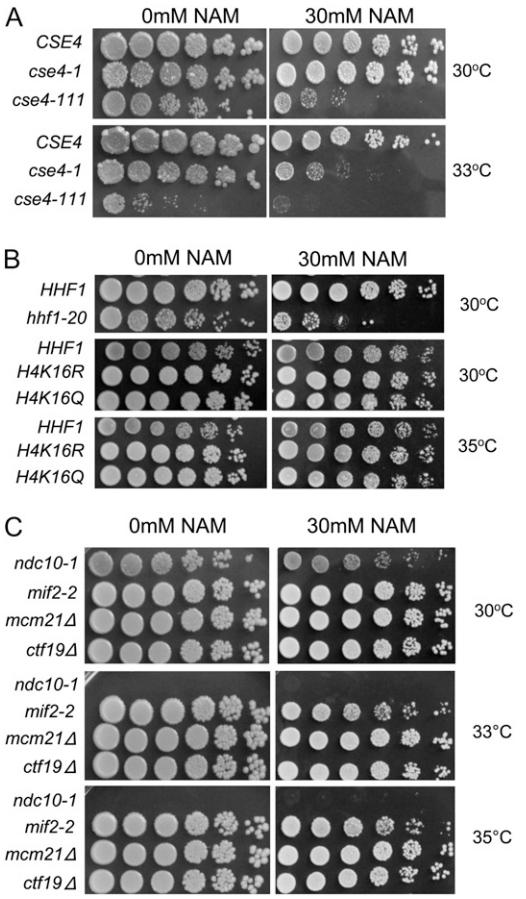

Figure 2 Kinetochore mutants are sensitized to nicotinamide (NAM). Strains were serially diluted fivefold and spotted onto YPD plates with 0 mM or 30 mM NAM, incubated at the indicated temperatures, and photographed after 3 days. (A) Wild-type *CSE4* (RC154) and temperature-sensitive C-terminal *cse4* mutants, *cse4-1* (RC147) and *cse4-111* (MSY1520). (B) Wild-type *HHF1* (MSY559) and temperature-sensitive chromosome segregation histone H4 mutant *hhf1-20* (MSY554) (top), and strains expressing wild-type histone H4 (YMB8155), nonacetylatable H4K16R (YMB8156), and acetylmimic H4K16Q (YMB8157) (middle and bottom). (C) Temperature-sensitive kinetochore mutants, *ndc10-1* (JK421), *mif2-2* (6849-10-1), and nonessential kinetochore mutants, *mcm21*Δ (YPH1715) and *ctf19*Δ (YPH1713). Note the *ndc10-1* mutant is inviable above 30°.

contain lower levels of H4K16Ac (~twofold less) similar to hypoacetylated HML (−CTL1) and *SPS22* (−CTL2) regions, previously reported to have low H4K16Ac (Liu *et al.* 2005), compared to *ARE1* (+CTL) (Figure 3B), a region with high levels of H4K16Ac (Liu *et al.* 2005). Similarly, we also observed low levels of H4K16Ac (approximately twofold less) at CEN VI compared to *ARE1* (+CTL) (Figure S4). Moreover, H4K16Ac levels are higher in the regions immediately upstream (~50 bp) and downstream (~400 bp) of CEN VI, which contains the *DEG1* and *LOC1* genes, respectively (Figure S5). These results show that H4K16 is hypoacetylated at centromeric chromatin and is not affected by the acetylation of neighboring genes. We note that while the *SNR189* region contains hyperacetylated H4, the level of acetylated H4K16 is lower compared to *ARE1* (Liu *et al.* 2005) and therefore, we have used *ARE1* as a positive control for H4K16 hyperacetylation rather than *SNR189*.

We have observed low levels of acetylated H4 at centromeres in the context of the endogenous chromosome and on a plasmid. The low level of acetylated centromeric H4 may be regulated by the kinetochore or associated proteins. To test this possibility, we sought to determine whether the hypoacetylated state of H4K16 is associated with noncentromeric regions containing Cse4p. In a recent report by Camahort *et al.* (2009) they found approximately four- to sixfold higher levels of Cse4p at rDNA (*NTS1-1* and *NTS1-2*) regions compared to loci where Cse4p is absent. We performed ChIP experiments to measure the levels of H4K16Ac at *NTS1-1* and *NTS1-2* and observed slightly less than twofold lower H4K16Ac compared to *ARE1* (Figure 3C), similar to the difference observed at CEN III (Figure 3B). We also observed enrichment for Cse4p at *NTS1-1* and *NTS1-2* consistent with that reported by Camahort *et al.* (2009) (Figure S6). These results suggest that acetylation of H4 may be dictated by association with Cse4p, or Cse4p tends to associate with genomic regions in which histone H4K16 is hypoacetylated.

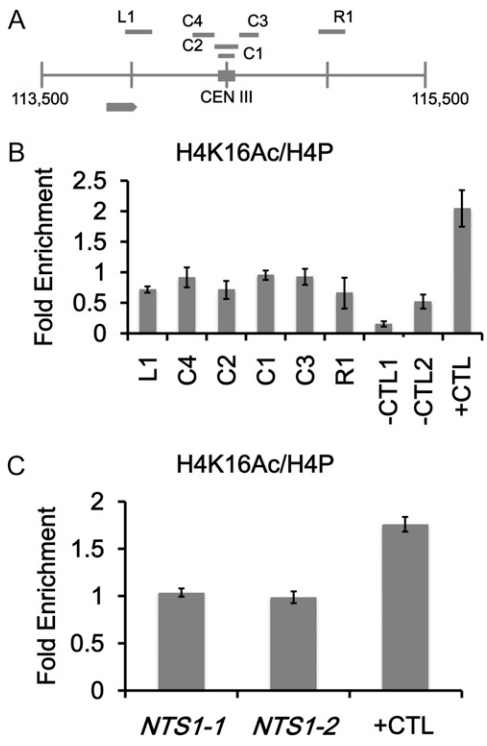

Figure 3 Low levels of H4K16Ac are present at the centromere and at noncentromeric loci enriched for Cse4p. ChIP experiments were performed with asynchronously grown wild-type strains (YMB6955 in B and YMB8077 in C). Immunoprecipitated DNA was subjected to quantitative PCR to determine enrichment for the indicated regions. (A) Diagram of CEN III (C1–4) and pericentromeric regions (L1 and R1) analyzed by ChIP. (B) ChIP experiments with antibodies to acetylated H4K16 (H4K16Ac) and pan H4 to measure levels of H4K16Ac and total H4 at C1–4 and at L1 and R1 or in C at *NTS1-1* and *NTS1-2* rDNA regions that contain Cse4p. HML (−CTL1) and *SPS22* (−CTL2) (Chr III: 42437–42630) serve as hypoacetylated and *ARE1* (+CTL) (Chr III: 212230–212450) serves as hyperacetylated H4K16 controls. Bar graphs show mean fold enrichment for H4K16Ac normalized to total H4 from three biological replicates with error bars showing standard error of the mean.

Centromeric H4K16 acetylation is increased in NAM treated cells

The increased sensitivity of *hhf1-20* and *cse4* mutants to NAM prompted us to examine whether NAM treatment affected the level of H4K16Ac at the centromere. We performed ChIP experiments with wild-type and *cse4-1* strains grown in 0 mM or 30 mM NAM. We observed an approximately twofold increase in centromeric H4K16Ac in wild-type and *cse4-1* strains grown in NAM compared to untreated cells (Figure 4, B and C). In addition, we also observed an increase in H4K16Ac at HML, which likely reflects a more general effect of NAM-mediated inhibition of NAD-dependent H4K16 deacetylation activity. These results show that NAM treatment causes an increase in H4K16 acetylation at the centromere and in combination with a kinetochore mutant (*cse4* and *hhf1-20*), results in growth defects.

Overexpression of SAS subunits is synthetic dosage lethal (SDL) in CSE4 and HHF1 mutants

Our ChIP experiments revealed that centromeric chromatin had lower levels of acetylated H4K16 and inhibiting HDACs with NAM led to loss of viability in kinetochore mutants. On the basis of these observations, we predict that increasing H4K16 histone acetyltransferase activity would exacerbate the growth defects in kinetochore mutants. To test this possibility, we determined whether overexpression of Sas2p (*GAL-SAS2*), an H4K16 histone acetyltransferase (HAT) (Shia *et al.* 2005) and Esa1p, an essential HAT that acetylates all four N-terminal histone H4 lysines (Smith *et al.* 1998; Allard *et al.* 1999), displayed genetic interactions in *cse4* and *hhf1* mutants. Indeed, we found that *cse4* mutants (*cse4-1* and *cse4-111*) with mutations in the C-terminal histone fold domain were sensitized to *GAL-SAS2* with the strongest effect at 35° and 33°, respectively (Figure 5, A and B). Moreover, overexpression of the Sas2p partners, Sas4p and Sas5p, also exhibited a SDL in *cse4-1* at 35° (Figure 5A). As previously reported, we also observed that overexpression of histone H4 suppresses the growth defect in

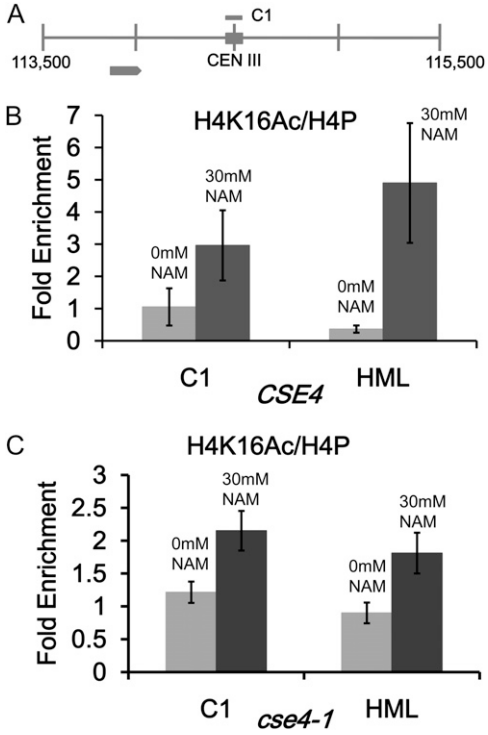

Figure 4 NAM causes an increase in centromeric H4K16Ac in wild-type and *cse4-1* strains. ChIP experiments were performed with *CSE4* (RC154) and *cse4-1* strains (RC147) grown in 0 mM or 30 mM NAM. Immunoprecipitated DNA was subjected to quantitative PCR to determine enrichment for H4K16Ac. (A) Diagram of CEN III and pericentromeric regions. (B) ChIP experiments with antibodies to H4K16Ac and pan H4 to measure levels of H4K16Ac at C1 in *CSE4* strains. (C) Same as B except in *cse4-1* strains. HML serves as a hypoacetylated H4K16 control region. Bar graphs show mean fold enrichment for H4K16Ac normalized to total H4 from three biological replicates with error bars showing standard error of the mean.

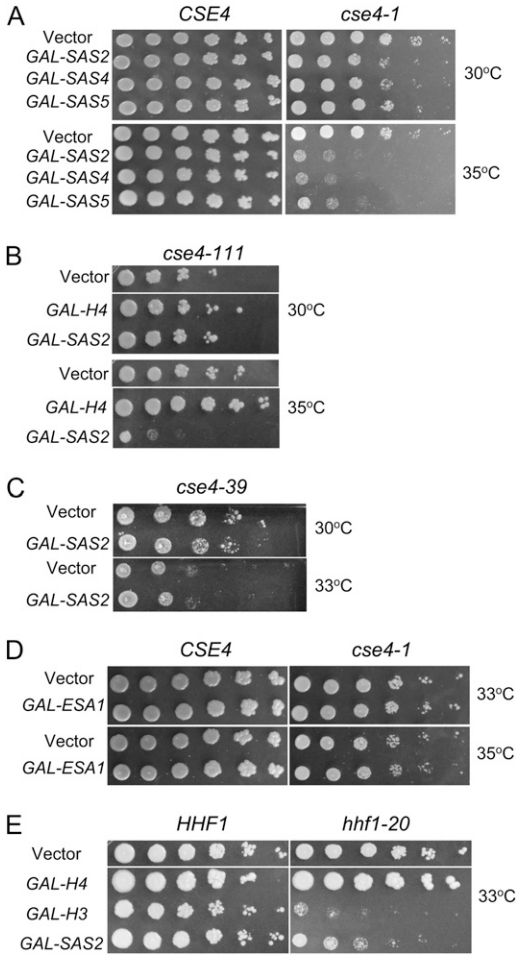

Figure 5 Overexpression of SAS subunits leads to SDL in kinetochore mutants. Strains were transformed with vector (vector) or vector containing the indicated gene under the Gal1 promoter (*GAL-*). Fivefold serial dilutions of each strain were spotted on SC −Ura plates containing 2% galactose and 2% raffinose, incubated at the indicated temperatures, and photographed after 3–5 days. (A) Wild-type *CSE4* (RC154) and C-terminal mutant *cse4-1* (RC147). (B) C-terminal mutant *cse4-111* (MSY1520). (C) N-terminal mutant *cse4-39* (YC190). (D) Wild-type *CSE4* (RC154) and C-terminal mutant *cse4-1* (RC147). (E) Wild-type *HHF1* (MSY559) and temperature-sensitive chromosome segregation mutant *hhf1-20* (MSY554) strains. Three or more independent transformants were tested for each experiment.

cse4-111 mutants (Figure 5B) (Glowczewski *et al.* 2000). However, there was no growth defect conferred by *GAL-SAS2* in *cse4-39* mutants, which have a mutation at the N-terminal domain of Cse4p (Figure 5C). We then tested the phenotypes of *ESA1* overexpression at 33° and 35° in *cse4-1* and observed no growth defect (Figure 5D). This is likely not due to a dominant negative effect, as we found no obvious differences in acetylated H4K16 protein levels in the presence or absence of *ESA1* overexpression in wild-type or *cse4-1* strains (Figure S7).

Considering that Cse4p binds to H4 to form the core centromeric nucleosome (Smith *et al.* 1996; Glowczewski *et al.* 2000; Furuyama and Biggins 2007), we tested whether *hhf1-20* was sensitized to *GAL-SAS2*. Consistent with previously published observations, we found that overexpression of histone H3 is SDL in *hhf1-20* (Figure 5E) (Glowczewski *et al.* 2000). Similar to the results in *cse4* mutants, *GAL-SAS2* exhibited SDL in an *hhf1-20* strain at 33°, compared to vector control (Figure 5E).

The SDL conferred by *GAL-SAS2* may be mediated by its catalytic or noncatalytic activity. To distinguish between these two possibilities, we expressed a *SAS2* catalytic mutant (*Gal-sas2m1*) in *cse4-1* and *cse4-111* mutants. The *sas2m1* allele encodes for a mutant protein that replaces residues 219–221 from GLG to AAA within the active site (Osada *et al.* 2001; Shia *et al.* 2005). Previous results have shown that the catalytic mutant, sas2m1p, displays a sixfold decrease in activity and is unable to complement a loss of silencing defect in *sas2Δ* mutants (Osada *et al.* 2001; Shia *et al.* 2005). Compared to wild-type *SAS2*, which causes a marked loss in viability in *cse4-1* and *cse4-111* at 33°, *GAL-sas2m1* had a reduced effect in these strains (Figure 6A).

Several reports have demonstrated that Scm3p binds to Cse4p and is required to maintain Cse4p at the centromere (Camahort *et al.* 2007; Mizuguchi *et al.* 2007; Stoler *et al.*

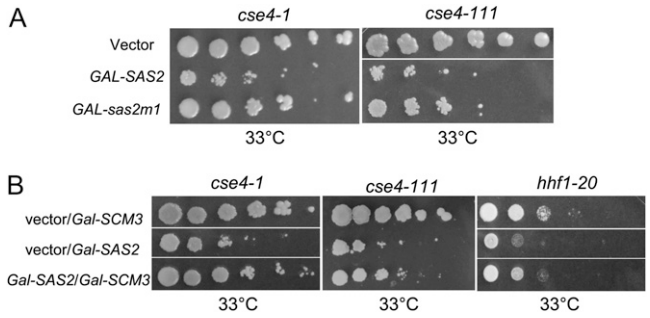

Figure 6 Catalytic activity of Sas2p contributes to SDL and *GAL-SCM3* suppresses the *GAL-SAS2* SDL. Strains were transformed with vector (vector) or vector containing the indicated gene under the Gal1 promoter (*GAL-*). Fivefold serial dilutions of each strain were spotted on SC −Ura plates containing 2% galactose and 2% raffinose, incubated at the indicated temperatures, and photographed after 3–5 days. (A) C-terminal mutants *cse4-1* (RC147) and *cse4-111* (MSY1520) strains, carrying vector, *GAL-SAS2*, or the catalytic mutant *GAL-sas2m1*. (B) C-terminal mutant *cse4-1*, *cse4-111*, and histone H4 mutant *hhf1-20* (MSY554) strains, carrying vector and *GAL-SCM3* or *GAL-SAS2* or carrying both *GAL-SAS2* and *GAL-SCM3*. At least three independent transformants were tested for each experiment.

2007). If the *SAS2* SDL is associated with disruption of the Cse4p-H4 complex then increasing the dosage of *SCM3* might suppress the loss in viability. Consistent with this prediction, we found that the SDL conferred by *SAS2* overexpression in *cse4-1*, *cse4-111*, and *hhf1-20* mutants was suppressed by overexpression of *SCM3* (Figure 6B). Taken together, these results suggest that SAS activity enhances the kinetochore defects in *cse4* C-terminal mutants and *hhf1-20* mutants.

Altered acetylation of histone H4 affects chromosome segregation

The observed lethality in kinetochore mutants overexpressing SAS subunits along with the reduced SDL displayed by the *SAS2* catalytic mutant suggest that increased H4K16 acetylation may lead to chromosome missegregation. To test this possibility, we determined the rate of chromosome loss in a reporter strain overexpressing *SAS2*, *SAS4*, and *SAS5*. Cells with a chromosome segregation defect lose the minichromosome and give rise to white colonies with red sectors (Hieter *et al.* 1985). Half-sectored colonies reflect chromosome loss within the first cell division. For example, a deletion of the spindle assembly checkpoint gene *MAD1* results in approximately eight half-sectored colonies per 1000 examined (Kastenmayer *et al.* 2005). We found an absence of half-sectored colonies for wild-type strains with vector alone or *Gal-SAS5* in ~1000 colonies, but observed half-sectored colonies for those expressing *GAL-SAS2* or *GAL-SAS4* (~1 or ~2.5 per 1000 colonies, respectively) (Figure 7A). We propose that the increased chromosome loss in *GAL-SAS4* might reflect the importance of this subunit for Sas2p activity as previously reported (Sutton *et al.* 2003).

The NAD-dependent deacetylases have been reported to deacetylate H4K16 to mediate silencing at the telomeres and the silent mating loci (Krebs 2007). Previous studies have shown that NAM inhibits Sir2p both *in vitro* and *in vivo* (Sanders *et al.* 2007). We predicted that inhibiting H4K16 deacetylation with NAM in combination with overexpression of *SAS2*, *SAS4*, and *SAS5* might enhance the rate of chromosome missegregation. Indeed, we found that addition of NAM resulted in increased chromosome loss in wild-type strains expressing *GAL-SAS2*, *GAL-SAS4*, and *GAL-SAS5* when compared to the vector control (~3, ~3.5, and ~2 per 1000 colonies, respectively) (Figure 7A).

If the enhanced chromosome loss defect conferred by NAM is in part through inhibition of *SIR2*, then deletion of *SIR2* or a *sir2-H364Y* catalytic mutant may lead to similar defects in chromosome segregation. We deleted *SIR2* in the reporter strain and transformed the strain with vector or vector containing either *sir2-H364Y* or wild-type *SIR2* and measured the number of half-sectored colonies as described for Figure 7A. We observed that the *sir2Δ* strain with either vector or *sir2-H364Y* displayed an increase in chromosome loss when compared to the strain with the complementing *SIR2* plasmid (~7–8 *vs.* <2 per 1000 colonies, respectively) (Figure 7B). These results show that the catalytic activity of Sir2p contributes to accurate chromosome segregation and

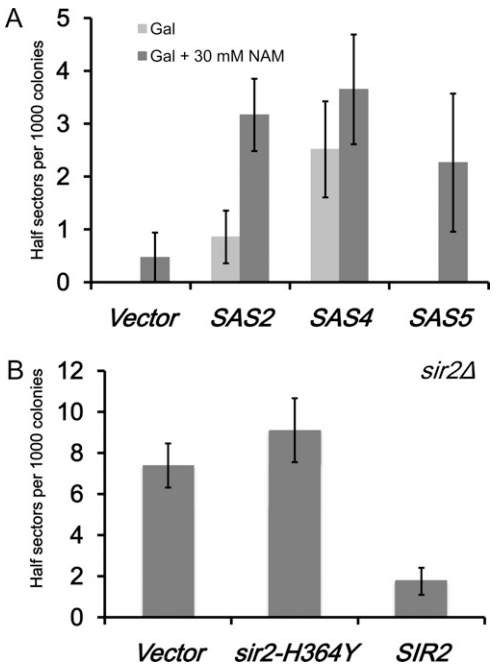

Figure 7 Altered H4K16Ac affects chromosome segregation. Chromosome loss assays were done with wild-type strains carrying a nonessential minichromosome (YPH1015) with vector or *SAS2*, *SAS4*, or *SAS5* expressed under the *GAL1* promoter. Loss of the minichromosome within the first cell division gives rise to colonies that are half red and half white. We measured colonies that were at least half red. (A) Bar graph showing the number of half-sectored colonies per 1000 for each strain on galactose media without (Gal) or with NAM (Gal + 30 mM NAM). (B) Bar graph shows the number of half-sectored colonies per 1000 for *SIR2* deletion strain (YMB7911) carrying pRS314 (vector), *sir2-H364Y* (catalytic mutant), or *SIR2*. Error bars show standard error of the mean from three biological replicates.

that deregulation of histone H4 acetylation leads to chromosome loss.

Histone H4K16Q acetylmimic mutant exhibits a chromosome loss phenotype

The observed growth and chromosome loss defects associated with altered H4 acetylation activity suggest that deregulated H4K16 acetylation may be the underlying cause for these phenotypes. To directly test this possibility, we created reporter strains that express either wild-type H4, H4K16R, which is nonacetylatable, or H4K16Q, an acetylmimic as the only forms of histone H4 and measured the rate of chromosome loss. We observed on average <1 half-sectored colony per 1000 for wild-type H4 and H4K16R strains (Figure 8). In contrast, H4K16Q mutants showed increased chromosome loss with an average ~4 half-sectored colonies per 1000 (Figure 8). Taken together, our results are consistent with the conclusion that acetylated lysine 16 on histone H4 may underlie the SAS-mediated SDL and sensitivity to NAM in *cse4-1* and *hhf1-20* strains and increased rate of chromosome loss in *sir2Δ*, *sir2-H364Y*, and wild-type cells treated with NAM.

Discussion

The function of histone H4 hypoacetylation in regional centromeres has remained an open question in chromosome biology. In this report, we show that hypoacetylated H4 is present at point centromeres in *S. cerevisiae* and that deregulation of H4 acetylation affects kinetochore function. We propose that hypoacetylated H4K16 is important for maintaining the integrity of the kinetochore and accurate chromosome segregation. That there were low levels of tAcH4, even at a minimal centromere flanked by heterologous sequences on a plasmid suggests that the kinetochore may contribute to the acetylation state of centromeric H4. On the basis of our results, we propose that H4K16 acetylation is a key modification that impacts kinetochore function and chromosome segregation. Our conclusion is supported by the following: (a) sensitivity of *cse4* and *hhf1* strains to NAM and SAS overexpression, (b) higher levels of centromeric H4K16Ac in wild-type and *cse4-1* strains treated with NAM, (c) increased chromosome loss in wild-type strains overexpressing subunits of the SAS complex, (d) increased chromosome loss in a *SIR2* deletion and *sir2-H364Y* catalytic mutant, and (e) increased chromosome loss in mutants expressing H4K16Q acetylmimic but not in H4K16R nonacetylatable mutants.

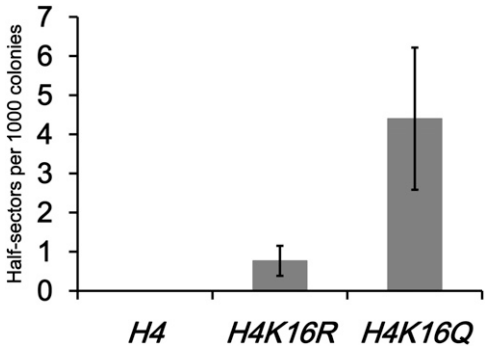

Figure 8 An H4K16Q acetylmimic mutant shows increased chromosome loss. Chromosome loss assays were performed with strains carrying a nonessential minichromosome that expresses wild-type H4 (YMB8155), H4K16R (YMB8156), or H4K16Q (YMB8157). Loss of the minichromosome within the first cell division gives rise to colonies that are half red and half white. We measured colonies that were at least half red. Bar graph shows the number of half-sectored colonies per 1000. Shown are results for three independent experiments and error bars show standard error of the mean.

We hypothesize that the Cse4p-H4 interactions within the histone fold domain of Cse4p plays a major role in protecting cells from the effects of high levels of histone acetylation. When these interactions are compromised, as in the *cse4* and *hhf1-20* mutants, a hypoacetylated N-terminal H4 becomes essential to maintain kinetochore integrity. This is supported by our results that showed both wild-type and *cse4-1* strains had an increase in centromeric acetylation of H4K16 when treated with NAM but unlike *cse4-1* and *hhf1-20* mutants, wild-type strains were not sensitive to NAM. Moreover, several kinetochore mutants (*ndc10-1*, *mif2-2*, *mcm21*, and *ctf19*) did not display growth defects when treated with NAM further supporting the hypothesis that the effects of NAM originate at the Cse4p-H4 complex. Similar to the results with NAM treatment, we propose that the phenotypes conferred by overexpression of SAS subunits are consistent with defects that originate at the Cse4p-H4 centromeric nucleosome. First, *SAS2* exhibited SDL in C-terminal *cse4* mutants (*cse4-1* and *cse4-111*) with defects in interactions with histone H4, but not an N-terminal *cse4* mutant (*cse4-39*). Second, overexpression of *SAS2* results in SDL in *hhf1-20* mutants that are predicted to have weakened interactions with Cse4p (Smith *et al.* 1996). Third, overexpression of *SCM3* suppressed the *SAS2* induced SDL in *cse4* and *hhf1-20* mutants. Scm3p, which coimmunoprecipitates with Cse4p, is required for kinetochore function and its overexpression suppresses temperature sensitivity of *cse4-1* strains (Camahort *et al.* 2007; Mizuguchi *et al.* 2007; Stoler *et al.* 2007). Suppression of the SAS SDL in *cse4* and *hhf1-20* by *SCM3* overexpression suggests that Scm3p might interact with Cse4p-H4 such that the nucleosome becomes protected from SAS-mediated acetylation, help recruit an H4 deacetylase to counteract the effects of SAS overexpression, or stabilizes mutant Cse4p interactions with H4.

A role for hypoacetylated histone H4 in chromosome segregation is further supported by our observations that *sir2Δ* and a *sir2-H364Y* catalytically inactive mutant exhibit increased chromosome loss rates. Previously, Sir2p was shown to be important for assembly of silent telomeric chromatin by deacetylation of H4K16 and Sas2p was necessary to restrict the spread of silenced chromatin into euchromatin (Kimura *et al.* 2002; Suka *et al.* 2002; Shia *et al.* 2006). In the absence of *SIR2*, *SAS2*-mediated acetylation of H4K16 occurs inappropriately at telomeres, thereby altering their

chromatin structure. Moreover, overexpression of *SIR2* has been reported to cause an increase in chromosome loss (Holmes *et al.* 1997). However, the mechanism of this defect is not understood. The phenotypes we observed for overexpression of *SAS2* might also reflect an imbalance with Sir2p activity leading to higher levels of acetylated H4K16. We hypothesize that Sir2p might act as the deacetylase that maintains low levels of centromeric acetylated H4K16. However, ChIP experiments revealed that Sir1p but not Sir2p, Sir3p, or Sir4p was present at the kinetochore (Sharp *et al.* 2003). Perhaps the association of Sir2p is weak and cannot be detected by ChIP or Sir2p might act on the Cse4p-H4 complex prior to centromeric assembly. Biochemical work demonstrated that Sir2p can deacetylate histone octamers and free histones, lending support for the latter possibility (Parsons *et al.* 2003). Sir2p has been shown to be important for transcriptional silencing within regional centromeric chromatin in *Drosophila*, but its effect on centromeric H4 and chromosome segregation has not been explored (Rosenberg and Parkhurst 2002). Given the role for *SIR2* at telomeres, it is possible that the chromosome loss phenotype of the *sir2* mutants may be due to telomeric dysfunction, which in turn leads to chromosome missegregation. While we cannot rule this out completely, we propose that our genetic analysis of *cse4* and *hhf1-20* mutants are consistent with centromeric-based defects due to altered histone acetylation.

Our genetic results with the catalytic mutant, *sas2m1*, the SDL conferred by overexpression of each of the SAS complex subunits, the loss of viability in *cse4* and *hhf1-20* mutants treated with NAM are all effects that support an H4K16 acetylation-based mechanism. To address this directly, we measured chromosome loss rates in H4K16R and H4K16Q mutants, in which K16 is nonacetylatable or mimics acetylation, respectively. Consistent with our hypothesis, we observed higher levels of chromosome loss in the H4K16Q strains compared to the H4K16R and wild-type H4 strains. We also showed a correlation between low levels of H4K16Ac and the presence of Cse4p at noncentromeric regions, suggesting that Cse4p either prefers to assemble with hypoacetylated H4 or the Cse4p-H4 complex is a substrate of deacetylases before or after nucleosome assembly. This is perhaps reminiscent of *trans*-histone modification pathways previously reported for canonical histones (Fingerman *et al.* 2007) and raises the possibility that a similar pathway may regulate modification of centromeric histone H4.

That we find wild-type cells remain relatively unaffected by altered HAT activity, while there is a severe loss in viability in kinetochore mutants, provides an exciting avenue for further research. Cancer therapies based on antimitotic drugs are being actively investigated (Jackson *et al.* 2007; Carpinelli and Moll 2009; Wood *et al.* 2010). On the basis of our work, combining HDAC inhibitors with drugs that compromise kinetochore function may provide a more efficacious approach to treat cancers with minimal effect on normal cells. Given the vast genetic tools in budding yeast, a comprehensive analysis of mitotic pathways that are vulnerable to altered H4 acetylation by small molecule HDAC inhibitors will facilitate the identification of potential targets for cancer therapy.

In summary, our work establishes that the point centromere of *S. cerevisiae* contains hypoacetylated H4. We show that hypoacetylated H4 at the centromere is a conserved feature in eukaryotes, despite having highly divergent centromeric sequences. Furthermore, our studies suggest that hypoacetylated H4K16 is important for kinetochore function and accurate chromosome segregation. While CenH3 alone cannot establish an active kinetochore in any system studied thus far, our results show a correlation between the acetylation state of H4 and regions of Cse4p association. Future studies will help understand whether the role for hypoacetylation of H4K16 in chromosome segregation is a conserved feature across all eukaryotic centromeres.

Acknowledgments

The authors thank S. Biggins, C. Chan, Danesh Moazed, J. Gerton, P. Megee, V. Measday, M. Smith, L. Pillus, and J. Workman for strains and plasmids. We are grateful to members of the Basrai lab, R. Baker, and D. Clarke for critical discussions and comments on the manuscript. This research was supported by the Intramural Research Program of the National Cancer Institute, National Institutes of Health.

Literature Cited

Allard, S., R. T. Utley, J. Savard, A. Clarke, P. Grant *et al.*, 1999 NuA4, an essential transcription adaptor/histone H4 acetyltransferase complex containing Esa1p and the ATM-related cofactor Tra1p. EMBO J. 18: 5108–5119.

Anderson, M., J. Haase, E. Yeh, and K. Bloom, 2009 Function and assembly of DNA looping, clustering, and microtubule attachment complexes within a eukaryotic kinetochore. Mol. Biol. Cell 20: 4131–4139.

Au, W. C., M. J. Crisp, S. Z. DeLuca, O. J. Rando, and M. A. Basrai, 2008 Altered dosage and mislocalization of histone H3 and Cse4p lead to chromosome loss in *Saccharomyces cerevisiae*. Genetics 179: 263–275.

Bloom, K. S., and J. Carbon, 1982 Yeast centromere DNA is in a unique and highly ordered structure in chromosomes and small circular minichromosomes. Cell 29: 305–317.

Bouck, D. C., and K. Bloom, 2007 Pericentric chromatin is an elastic component of the mitotic spindle. Curr. Biol. 17: 741–748.

Bouck, D. C., A. P. Joglekar, and K. S. Bloom, 2008 Design features of a mitotic spindle: balancing tension and compression at a single microtubule kinetochore interface in budding yeast. Annu. Rev. Genet. 42: 335–359.

Camahort, R., B. Li, L. Florens, S. K. Swanson, M. P. Washburn *et al.*, 2007 Scm3 is essential to recruit the histone H3 variant Cse4 to centromeres and to maintain a functional kinetochore. Mol. Cell 26: 853–865.

Camahort, R., M. Shivaraju, M. Mattingly, B. Li, S. Nakanishi *et al.*, 2009 Cse4 is part of an octameric nucleosome in budding yeast. Mol. Cell 35: 794–805.

Carpinelli, P., and J. Moll, 2009 Is there a future for Aurora kinase inhibitors for anticancer therapy? Curr. Opin. Drug Discov. Devel. 12: 533–542.

Crotti, L. B., and M. A. Basrai, 2004 Functional roles for evolutionarily conserved Spt4p at centromeres and heterochromatin in *Saccharomyces cerevisiae*. EMBO J. 23: 1804–1814.

Dang, W., K. K. Steffen, R. Perry, J. A. Dorsey, F. B. Johnson *et al.* 2009 Histone H4 lysine 16 acetylation regulates cellular lifespan. Nature. 459: 802–807.

Ekwall, K., 2007 Epigenetic control of centromere behavior. Annu. Rev. Genet. 41: 63–81.

Fingerman, I. M., H. C. Li, and S. D. Briggs, 2007 A charge-based interaction between histone H4 and Dot1 is required for H3K79 methylation and telomere silencing: identification of a new trans-histone pathway. Genes Dev. 21: 2018–2029.

Furuyama, S., and S. Biggins, 2007 Centromere identity is specified by a single centromeric nucleosome in budding yeast. Proc. Natl. Acad. Sci. USA 104: 14706–14711.

Gelperin, D. M., M. A. White, M. L. Wilkinson, Y. Kon, L. A. Kung *et al.* 2005 Biochemical and genetic analysis of the yeast proteome with movable ORF collection. Genes Dev. 23: 2816–2826.

Glowczewski, L., P. Yang, T. Kalashnikova, M. S. Santisteban, and M. M. Smith, 2000 Histone-histone interactions and centromere function. Mol. Cell. Biol. 20: 5700–5711.

Hayashi, T., Y. Fujita, O. Iwasaki, Y. Adachi, K. Takahashi *et al.*, 2004 Mis16 and Mis18 are required for CENP-A loading and histone deacetylation at centromeres. Cell 118: 715–729.

Hieter, P., C. Mann, M. Snyder, and R. W. Davis, 1985 Mitotic stability of yeast chromosomes: a colony color assay that measures nondisjunction and chromosome loss. Cell 40: 381–392.

Holmes, S. G., A. B. Rose, K. Steuerle, E. Saez, S. Sayegh *et al.*, 1997 Hyperactivation of the silencing proteins, Sir2p and Sir3p, causes chromosome loss. Genetics 145: 605–614.

Jackson, J. R., D. R. Patrick, M. M. Dar, and P. S. Huang, 2007 Targeted anti-mitotic therapies: Can we improve on tubulin agents? Nat. Rev. Cancer 7: 107–117.

Kanta, H., L. Laprade, A. Almutairi, and I. Pinto, 2006 Suppressor analysis of a histone defect identifies a new function for the Hda1 complex in chromosome segregation. Genetics 173: 435–450.

Karpen, G. H., and R. C. Allshire, 1997 The case for epigenetic effects on centromere identity and function. Trends Genet. 13: 489–496.

Kastenmayer, J. P., M. S. Lee, A. L. Hong, F. A. Spencer, and M. A. Basrai, 2005 The C-terminal half of *Saccharomyces cerevisiae* Mad1p mediates spindle checkpoint function, chromosome transmission fidelity and CEN association. Genetics 170: 509–517.

Kimura, A., T. Umehara, and M. Horikoshi, 2002 Chromosomal gradient of histone acetylation established by Sas2p and Sir2p functions as a shield against gene silencing. Nat. Genet. 32: 370–377.

Krebs, J. E., 2007 Moving marks: dynamic histone modifications in yeast. Mol. Biosyst. 3: 590–597.

Liu, C. L., T. Kaplan, M. Kim, S. Buratowski, S. L. Schreiber *et al.*, 2005 Single-nucleosome mapping of histone modifications in *S. cerevisiae*. PLoS Biol. 3: e328.

Millar, C. B., and M. Grunstein, 2006 Genome-wide patterns of histone modifications in yeast. Nat. Rev. Mol. Cell Biol. 7: 657–666.

Mizuguchi, G., H. Xiao, J. Wisniewski, M. M. Smith, and C. Wu, 2007 Nonhistone Scm3 and histones CenH3–H4 assemble the core of centromere-specific nucleosomes. Cell 129: 1153–1164.

Osada, S., A. Sutton, N. Muster, C. E. Brown, J. R. Yates 3rd *et al.*, 2001 The yeast SAS (something about silencing) protein complex contains a MYST-type putative acetyltransferase and functions with chromatin assembly factor Asf1. Genes Dev. 15: 3155–3168.

Parsons, X. H., S. N. Garcia, L. Pillus, and J. T. Kadonaga, 2003 Histone deacetylation by Sir2 generates a transcriptionally repressed nucleoprotein complex. Proc. Natl. Acad. Sci. USA 100: 1609–1614.

Rosenberg, M. I., and S. M. Parkhurst, 2002 *Drosophila* Sir2 is required for heterochromatic silencing and by euchromatic Hairy/E(Spl) bHLH repressors in segmentation and sex determination. Cell 109: 447–458.

Rusche, L. N., A. L. Kirchmaier, and J. Rine, 2003 The establishment, inheritance, and function of silenced chromatin in *Saccharomyces cerevisiae*. Annu. Rev. Biochem. 72: 481–516.

Sanders, B. D., K. Zhao, J. T. Slama, and R. Marmorstein, 2007 Structural basis for nicotinamide inhibition and base exchange in Sir2 enzymes. Mol. Cell 25: 463–472.

Saunders, M.J., E. Yeh, M. Grunstein, and K. Bloom, 1990 Nucleosome depletion alters the chromatin structure of *Saccharomyces cerevisiae* centromeres. Mol. Cell. Biol. 10: 5721–5727.

Shahbazian, M. D., and M. Grunstein, 2007 Functions of site-specific histone acetylation and deacetylation. Annu. Rev. Biochem. 76: 75–100.

Sharp, J. A., A. A. Franco, M. A. Osley, and P. D. Kaufman, 2002 Chromatin assembly factor I and Hir proteins contribute to building functional kinetochores in *S. cerevisiae*. Genes Dev. 16: 85–100.

Sharp, J. A., D. C. Krawitz, K. A. Gardner, C. A. Fox, and P. D. Kaufman, 2003 The budding yeast silencing protein Sir1 is a functional component of centromeric chromatin. Genes Dev. 17: 2356–2361.

Shia, W. J., S. Osada, L. Florens, S. K. Swanson, M. P. Washburn *et al.*, 2005 Characterization of the yeast trimeric-SAS acetyltransferase complex. J. Biol. Chem. 280: 11987–11994.

Shia, W. J., B. Li, and J. L. Workman, 2006 SAS-mediated acetylation of histone H4 Lys 16 is required for H2A.Z incorporation at subtelomeric regions in *Saccharomyces cerevisiae*. Genes Dev. 20: 2507–2512.

Shogren-Knaak, M., and C. L. Peterson, 2006 Switching on chromatin: mechanistic role of histone H4–K16 acetylation. Cell Cycle 5: 1361–1365.

Sikorski, R. S., and P. Hieter, 1989 A system of shuttle vectors and yeast host strains designed for efficient manipulation of DNA in Saccharomyces cerevisiae Genetics 122: 19–27.

Smith, E. R., A. Eisen, W. Gu, M. Sattah, A. Pannuti *et al.*, 1998 ESA1 is a histone acetyltransferase that is essential for growth in yeast. Proc. Natl. Acad. Sci. USA 95: 3561–3565.

Smith, M. M., P. Yang, M. S. Santisteban, P. W. Boone, A. T. Goldstein *et al.*, 1996 A novel histone H4 mutant defective in nuclear division and mitotic chromosome transmission. Mol. Cell. Biol. 16: 1017–1026.

Stoler, S., K. C. Keith, K. E. Curnick, and M. Fitzgerald-Hayes, 1995 A mutation in *CSE4*, an essential gene encoding a novel chromatin-associated protein in yeast, causes chromosome nondisjunction and cell cycle arrest at mitosis. Genes Dev. 9: 573–586.

Stoler, S., K. Rogers, S. Weitze, L. Morey, M. Fitzgerald-Hayes *et al.*, 2007 Scm3, an essential *Saccharomyces cerevisiae* centromere protein required for G2/M progression and Cse4 localization. Proc. Natl. Acad. Sci. USA 104: 10571–10576.

Strahl, B. D., and C. D. Allis, 2000 The language of covalent histone modifications. Nature 403: 41–45.

Suka, N., K. Luo, and M. Grunstein, 2002 Sir2p and Sas2p opposingly regulate acetylation of yeast histone H4 lysine16 and spreading of heterochromatin. Nat. Genet. 32: 378–383.

Sullivan, B. A., and G. H. Karpen, 2004 Centromeric chromatin exhibits a histone modification pattern that is distinct from both euchromatin and heterochromatin. Nat. Struct. Mol. Biol. 11: 1076–1083.

Sutton, A., W. J. Shia, D. Band, P. D. Kaufman, S. Osada *et al.*, 2003 Sas4 and Sas5 are required for the histone acetyltransferase activity of Sas2 in the SAS complex. J. Biol. Chem. 278: 16887–16892.

Tanny, J. C., D. S. Kirkpatrick, S. A. Gerber, S. P. Gygi, and D. Moazed, 2004 Budding yeast silencing complexes and regulation of Sir2 activity by protein-protein interactions. Mol. Cell Biol. 16: 6931–6946.

Wang, Z., D. E. Schones, and K. Zhao, 2009 Characterization of human epigenomes. Curr. Opin. Genet. Dev. 19: 127–134.

Wood, K. W., L. Lad, L. Luo, X. Qian, S. D. Knight *et al.*, 2010 Antitumor activity of an allosteric inhibitor of centromere-associated protein-E. Proc. Natl. Acad. Sci. USA 107: 5839–5844.

Yeh, E., J. Haase, L. V. Paliulis, A. Joglekar, L. Bond *et al.*, 2008 Pericentric chromatin is organized into an intramolecular loop in mitosis. Curr. Biol. 18: 81–90.

Communicating editor: N. M. Hollingsworth

GENETICS

Supporting Information
http://www.genetics.org/content/suppl/2011/06/06/genetics.111.130781.DC1

A Role for Histone H4K16 Hypoacetylation in *Saccharomyces cerevisiae* Kinetochore Function

John S. Choy, Rachel Acuña, Wei-Chun Au, and Munira A. Basrai

DOI: 10.1534/genetics.111.130781

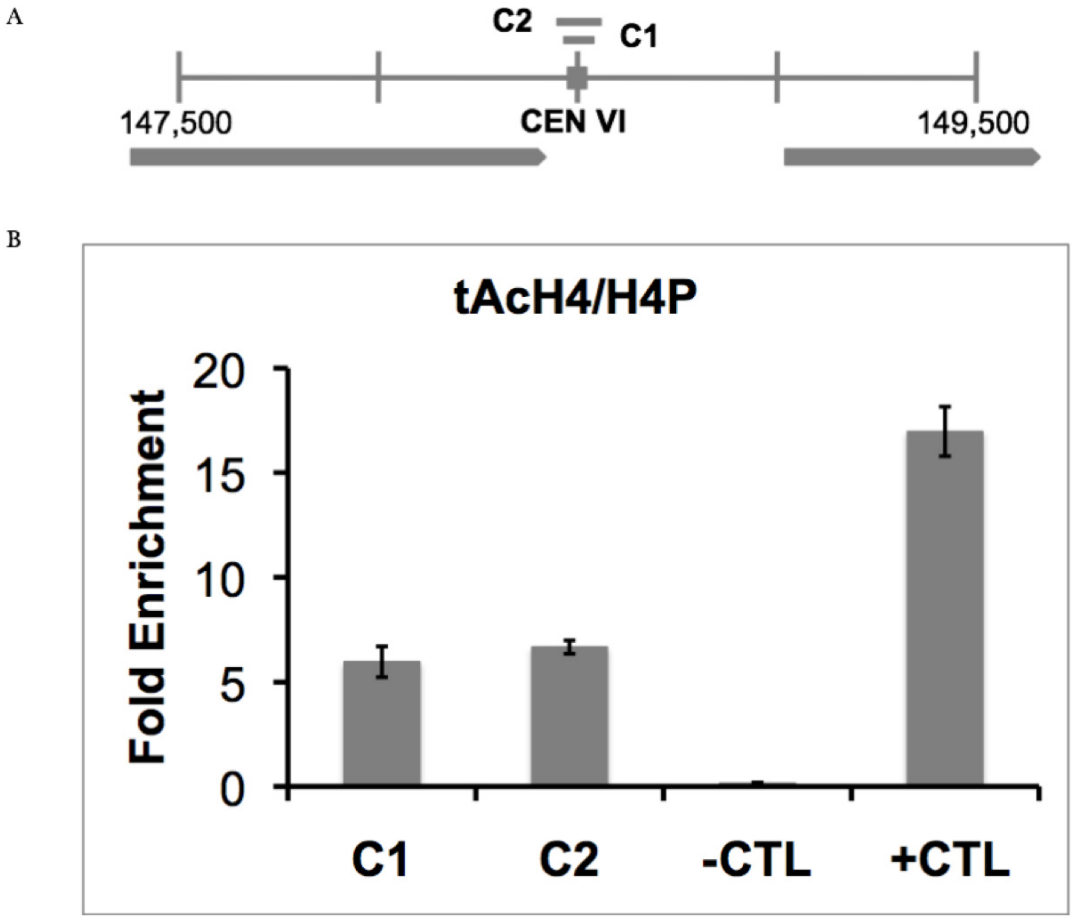

Figure S1 Low Levels of tetra-acetylated H4 are Observed at CEN VI. Chromatin immunoprecipitation (ChIP) experiments were performed with asynchronously grown wild type strains expressing Myc-Cse4p (YMB6955). (A) Diagram of CEN (C1-2) on chromosome VI analyzed by ChIP. Solid square represents the CEN VI sequence and each vertical line from chromosomal coordinate 147,500 to 149,500 denotes 500bp increments. Grey arrows represent *DEG1* and *LOC1* genes upstream and downstream of CEN VI, respectively. (B) ChIP with antibodies to acetylated histone H4 (tAcH4) to measure the levels of H4 acetylation. HML (-CTL) serves as a hypoacetylated H4 control and *SNR189* (+CTL) (Chr III: 178729-178589) is a hyperacetylated H4 control. ChIP for total H4 was performed with antibodies to pan H4 (H4P) that recognize modified and unmodified forms. Bar graphs show mean fold enrichment for tAcH4 normalized to total H4 from three biological replicates, with error bars showing standard error of the mean.

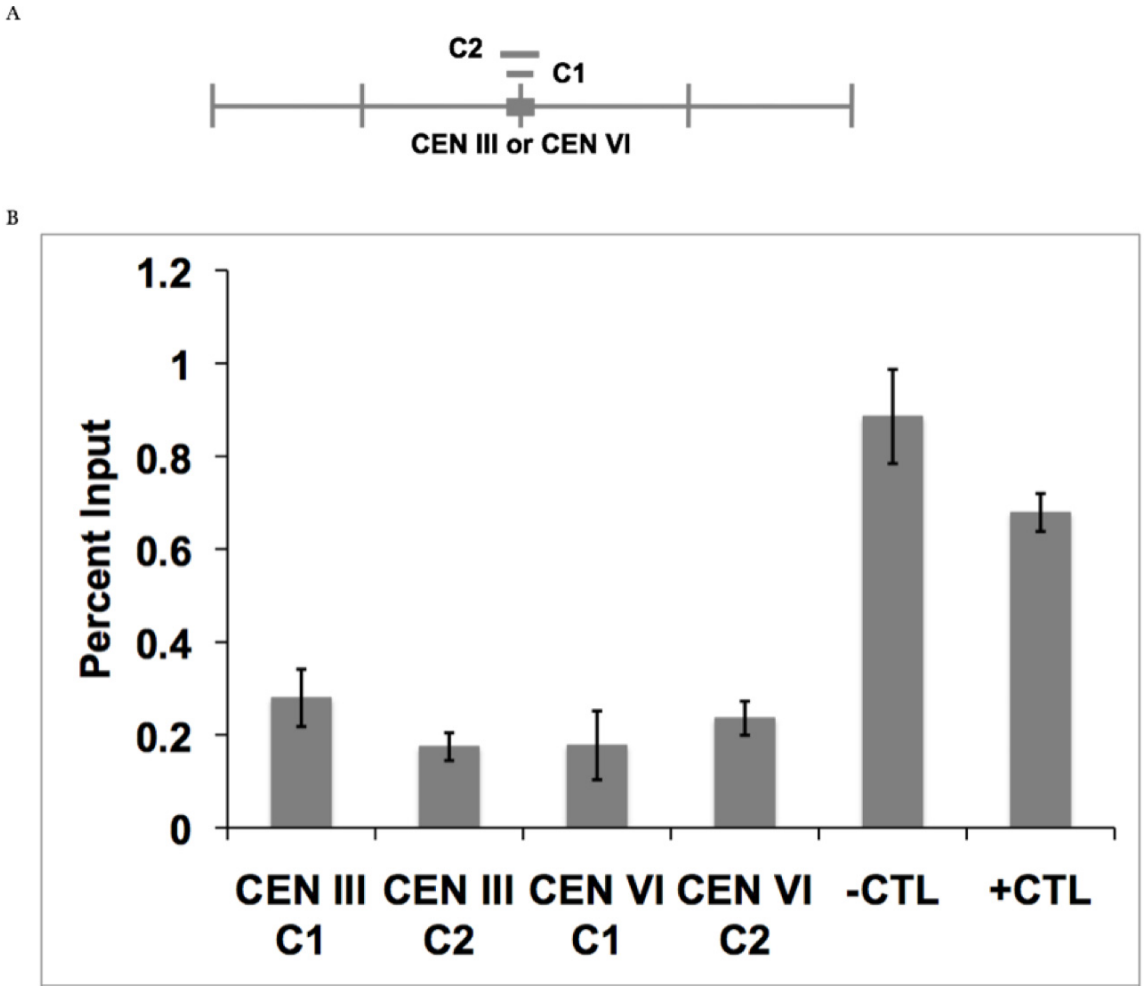

Figure S2 Differences in Chromatin immunoprecipitation (ChIP) efficiencies for pan-H4 between centromeric and non-centromeric regions. ChIP experiments were performed with asynchronously grown wild type strains (YMB6955). (A) Diagram of CEN (C1-2) on chromosome III or VI analyzed by ChIP. Solid square represents the CEN sequence and each vertical line denotes 500bp increments. (B) ChIP with antibodies to pan H4 (H4P) that recognizes modified and unmodified forms of H4 for the indicated regions (centromeric - C1-2), non-centromeric regions, HML – region that contains hypoacetylated H4K16 (-CTL), and *ARE1* – region that contains hyperacetylated H4K16 (+CTL). Bar graphs show mean percent input for three biological replicates, with error bars showing standard error of the mean.

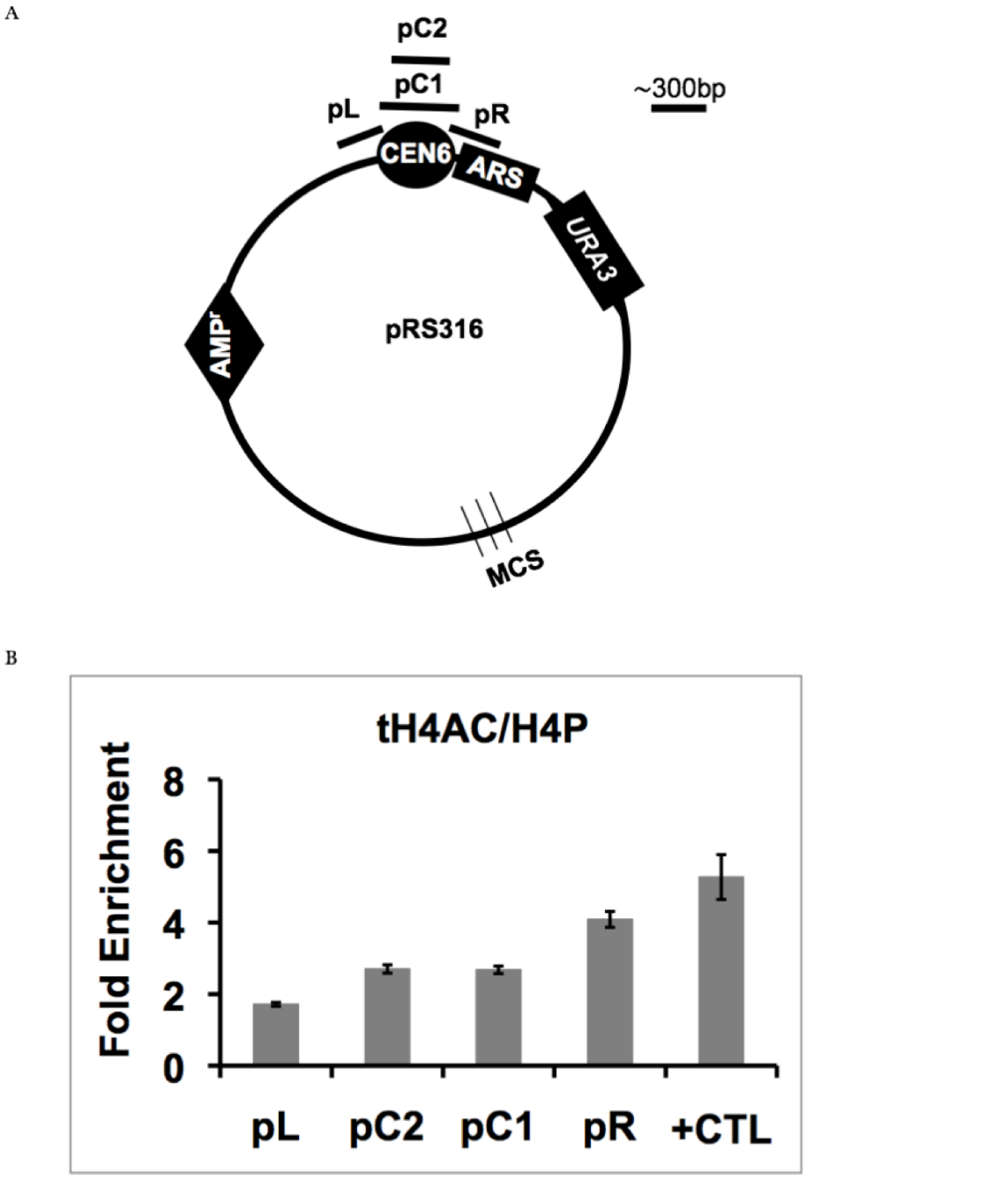

Figure S3 Low Levels of acetylated H4 are Observed at a plasmid CEN. (A) Diagram showing regions analyzed on a plasmid centromere that is identical to CEN VI. To specifically ChIP tAcH4 at plasmid CEN VI the chromosomal CEN VI was replaced with CEN XI in an otherwise wild type strain (YMB511). (B) ChIP with antibodies to tetra-acetylated histone H4 (tAcH4) to measure the levels of tAcH4 at plasmid centromeric (pC1-pC2) and pericentromeric regions (pL and pR). *SNR189* region that contains hyperacetylated H4 serves as a positive control (+CTL). Standard PCR was performed followed by agarose gel electrophoresis and quantification of DNA products stained with EtBr. Bar graphs show mean fold enrichment for tAcH4 normalized to total H4 from three biological replicates, with error bars showing standard error of the mean.

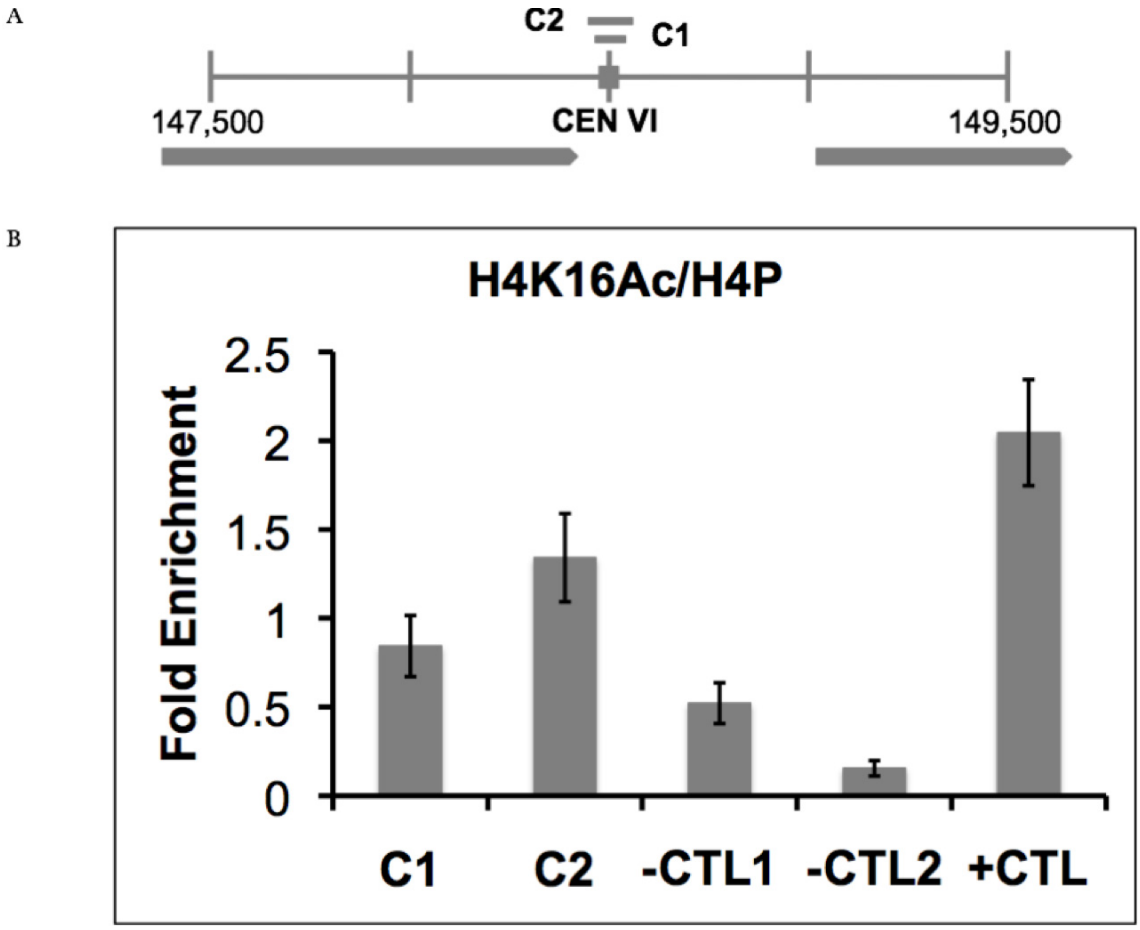

Figure S4 Low Levels of H4K16Ac are Observed at CEN VI. ChIP experiments were performed with asynchronously grown wild type strains expressing Myc-Cse4p (YMB6955). (A) Diagram of CEN (C1-2) on chromosome VI analyzed by ChIP. Solid square represents the CEN VI sequence and each vertical line from chromosomal coordinate 147,500 to 149,500 denotes 500bp increments. Grey arrows represent *DEG1* and *LOC1* genes upstream and dpwnstream of CEN VI, respectively. (B) ChIP to measure the levels of acetylated H4K16 (H4K16Ac) with antibodies to H4K16Ac. HML (-CTL1) and *SPS22* (-CTL2) (Chr III: 42437-42630) serve as hypoacetylated H4 controls and *ARE1* (+CTL) (Chr III: 212230-212450) serves as a hyperacetylated H4K16 control. ChIP for total H4 was performed with antibodies to pan H4 (H4P) that recognize modified and unmodified forms. Bar graphs show mean fold enrichment for H4K16Ac normalized to total H4 from three biological replicates, with error bars showing standard error of the mean.

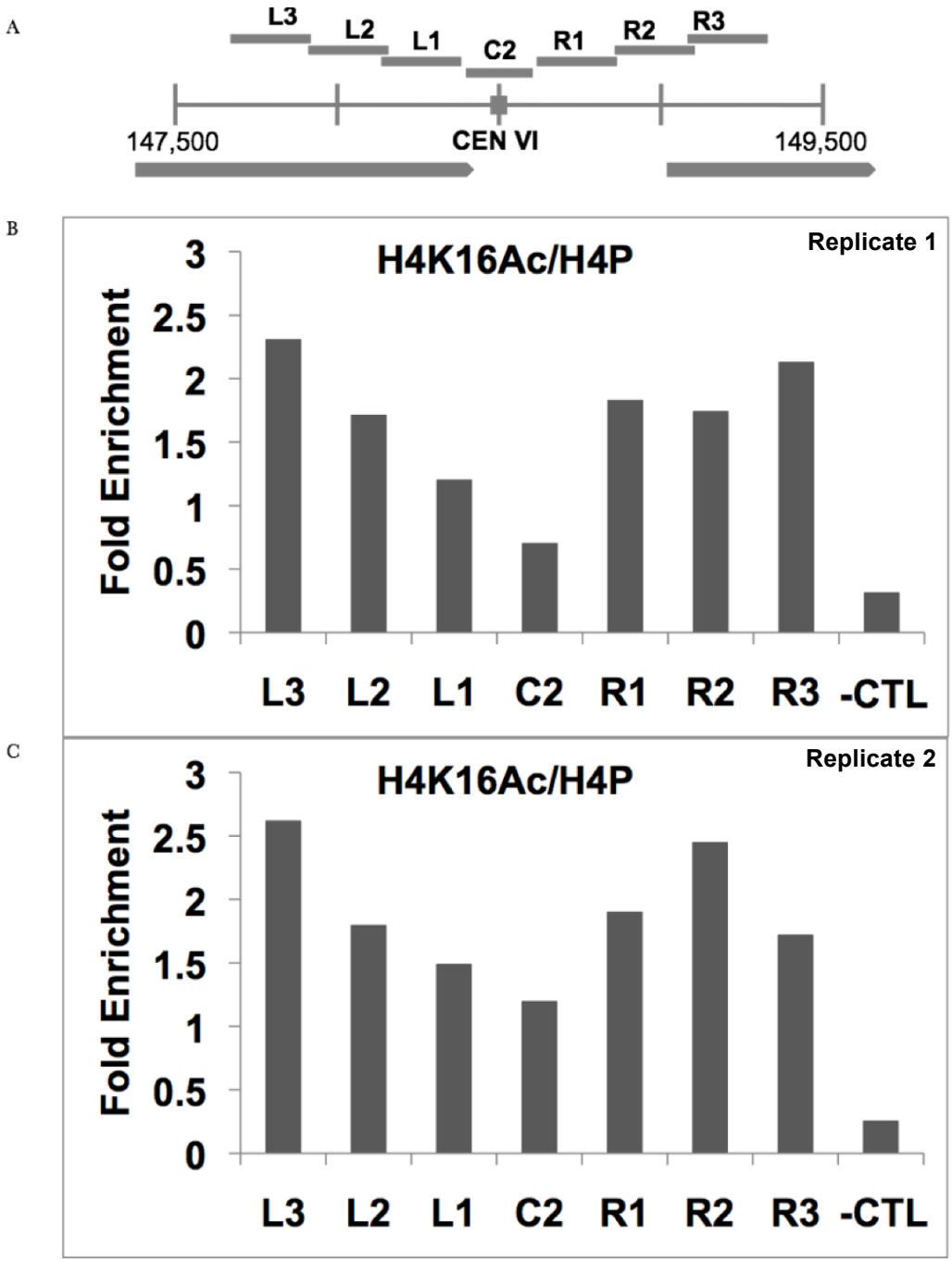

Figure S5 Regions that overlap with *DEG1* and *LOC1* have higher levels of H4K16Ac compared to the centromere. ChIP experiments were performed with asynchronously grown wild type strains expressing (YMB6955). (A) Diagram of CEN VI (C2) and flanking regions that overlap with *DEG1* (L1-3) and *LOC1* (R1-3) present on chromosome VI analyzed by ChIP. Solid square represents the CEN VI sequence and each vertical line from chromosomal coordinate 147,500 to 149,500 denotes 500bp increments. Grey arrows represent *DEG1* and *LOC1* genes upstream and downstream of CEN VI, respectively. (B and C) ChIP to measure the levels of acetylated H4K16 (H4K16Ac) with antibodies to H4K16Ac. HML (-CTL) serves as a hypoacetylated H4 controls. ChIP for total H4 was performed with antibodies to pan H4 (H4P) that recognize modified and unmodified forms. Bar graphs show fold enrichment for H4K16Ac normalized to total H4. B and C are two biological replicates.

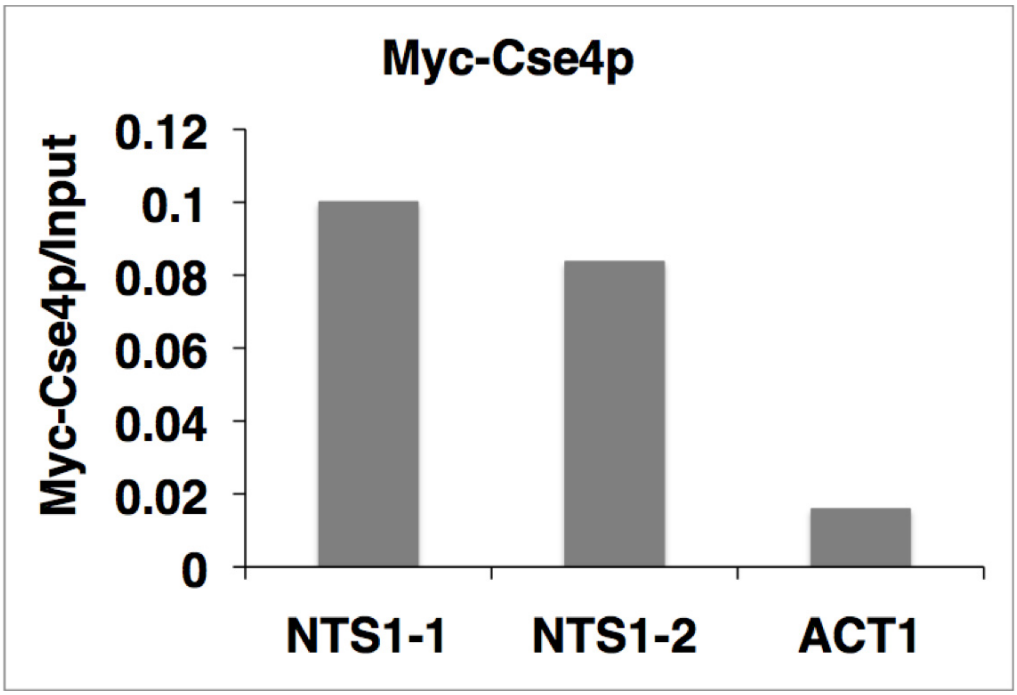

Figure S6 Myc-Cse4 is enriched at non-centromeric loci, *NTS1-1* and *NTS1-2*. *NTS1-1* and *NTS1-2* regions have been reported to be enriched with Cse4p. ChIP experiments were performed to measure levels of Cse4p at these regions with asynchronously grown wild type strains that carry Myc-Cse4 under its own promoter. *ACT1* region serves as a negative control as it has previously been reported that Cse4p is not enriched at this locus (Au et al. 2008). Anti-Myc antibodies were used for ChIP experiments followed by standard PCR with agarose gel electrophoresis and quantification of DNA products stained with EtBr. Bar graphs show fold enrichment for Myc-Cse4 normalized to input.

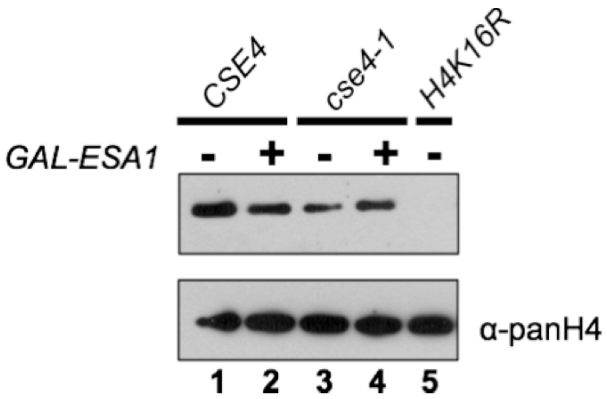

Figure S7 Total levels of acetylated H4K16 in *CSE4* and *cse4-1* strains overexpressing *ESA1* are similar. Western blotting was performed with whole cell protein extracts of *CSE4* (YMB6955) and *cse4-1* (YMB6917) strains carrying vector alone (-) lanes 1 and 3 or *Gal-ESA1* (+) lanes 2 and 4 grown in SC-URA with 2% galactose and 2% raffinose. Anti-acetylated H4K16 and anti-pan H4 antibodies were used to detect acetylated H4K16 (top) or total H4 (modified and unmodified) (bottom). Protein extract from H4K16R (lane 5) was used as a control to show that the anti-acetylated H4K16 antibody recognizes the acetylated form of H4K16. Protein extracts were prepared as described in (Kushnirov , V. V., 2000 Rapid and reliable protein extraction from 11 yeast. Yeast 16: 857-860)

Table S1 Description of yeast strains

Strain	Genotype	Reference
6849-10-1	*MATa ura3-52 mif2-3*	Brown et al., 1993
JK421	*MATa ade2-1 ura3-1 his3-11,1 trp1-1 leu2-3, 112 can1-100 ndc10-1*	Goh & Kilmartin, 1993
MSY554	*MATa ura3-52 leu2-3, 112 lys2Δ200 HHT1hhf1-20 Δ(HHT1-HHF1) Δ(HHT2-HHF2)*	Glowczewski et al., 2000
MSY559	*MATa ura3-52 leu2-3, 112 lys200 HHT1HHF1 Δ(HHT2-HHF2)*	Glowczewski et al., 2000
MSY1519	*MATa ade2 can1-100 his3-11, 15 leu2-3, 112 trp1-1, ura3-1 CSE4::LEU2 + HA-cse4-110-TRP*	Glowczewski et al., 2000
MSY1520	*MATa ade2 can1-100 his3-11, 15 leu2-3, 112 trp1-1, ura3-1 CSE4::LEU2 + HA-cse4-111-TRP1*	Glowczewski et al., 2000
RC147	*MATa ura3-1 leu2,3-112 trp1-1 ade2-1 can1-100 cse4-1 Δbar1 SCM3-3FLAG::KAN, NDC10-13Myc::TRP1*	Camahort et al., 2007
RC154	*MATa ura3-1 leu2,3-112 trp1-1 ade2-1 can1-100 Δbar1 SCM3-3FLAG::KAN NDC10-12MYC::TRP1*	Camahort et al., 2007
YC190	*MATa ade2-101 ade3-24 his11, 15 leu2-3 trp1-Δ901 ura3-52 cse4-39::TRP1*	Chen et al., 2000
YMB6955	*MATa ura3-1 leu2,3-112 trp1-1 ade2-1 can1-100 Δbar1 SCM3-3FLAG::KAN, cse4-12MYC::HIS3*	This Study
YMB7911	Same as YPH1015 with *sir2Δ::kanMX*	This study
YMB8077	Same as YPH1015 without CF*111*, *cen6::CEN11-LEU2*, pRS316	This study
YPH1015	*MATa ura3-52 lys2-801 ade2-101 trp1-Δ63 his3-Δ200 leu2-Δ1 CF111 (CEN3.L.YPH983) HIS3 SUP11*	Connelly & Hieter, 1996
YPH1713	*MATa mfa1Δ::MFA1pr-LEU2 can1Δ MFA1pr-HIS3 ura3Δ leu2Δ his3 trpΔ ctf19:: NatMX4*	Measday et al., 2005
YMB8155	*MATa ura3-52 lys2-801 ade2-101 trp1-Δ63 his3-Δ200 leu2-Δ1 CF111 (CEN3.L.YPH983) HIS3 SUP11 hht1-hhf1::NatMX4 hht2-hhf2::[H3-H4]-URA3*	This Study
YMB8156	*MATa ura3-52 lys2-801 ade2-101 trp1-Δ63 his3-Δ200 leu2-Δ1 CF111 (CEN3.L.YPH983) HIS3 SUP11 hht1-hhf1::NatMX4 hht2-hhf2::[H3-H4K16R]-URA3*	This Study
YMB8157	*MATa ura3-52 lys2-801 ade2-101 trp1-Δ63 his3-Δ200 leu2-Δ1 CF111 (CEN3.L.YPH983) HIS3 SUP11 hht1-hhf1::NatMX4 hht2-hhf2::[H3-H4K16Q]-URA3*	This Study